

# MAELab: a framework to automatize landmarks setting

LE Van Linh	BEURTON-AIMAR Marie	KRAHENBUHL Adrien	PARISEY Nicolas
LaBRI-CNRS 5800 ITDLU, Dalat Univ-V linhlv@dlu.edu.vn/ van-linh.le@labri.fr	LaBRI-CNRS 5800 Bordeaux University 33400 Talence-F beurton@labri.fr	LaBRI-CNRS 5800 Bordeaux University 33400 Talence-F adrien.krahenbuhl@labri.fr	IGEPP INRA 1349 35653 Le Rheu-F nparisey@rennes.inra.fr

## Abstract

Phenotype of insect species are characterized by several informations like age, sex, morphological measures or environmental parameters. Biologists are familiar to manually get morphological measures and in the case of analysis at the macro level (tissues, small parts of the animal ...) they can do directly by measuring the element geometry: length, width, diameter, angles, .... Another way to obtain morphological measures is to take pictures of these elements and to run image processing algorithms. In order to evaluate a population of beetles into Brittany lands, a collection of 293 beetles has been built. For each beetle, the images of the left and right mandibles are available and a set of 16 and 18 landmarks (resp. left and right) have been manually set, given the ground truth to compare to the estimated landmarks. In a previous work [4] based on Palaniswamy article [6], we have shown that the probabilistic Hough Transform (PHT) can provide very interesting results if we consider the centroid measure of the mandible as the parameter to obtain. But if the goal is to consider more precisely the position or the geometry of landmark areas, the results are not accurate enough to consider the estimated landmarks instead of manual landmarks. In this paper, we have improved the previous algorithms of segmentation based on Canny algorithm, and we have preferred a registration procedure based on an iteration of the Principal Component Analysis calculus. To achieve the estimated landmarks setting we have computed a SIFT descriptor limited to the landmarks area in the model and correlated it to the scene image. A workflow, MAELab, has been written, containing all the operations; it is freely available as library functions on a GitHub website.

## Keywords

Automatic morphology, landmarks identification, image registration.

## 1 INTRODUCTION

In biology, morphology analysis is widely used to keep the changing information of the organism or detecting the difference information between the organisms. From the result of morphology analysis, we can determine the evolution of an organism family, or we may classify the organisms. Especially in agriculture, morphology is one of best ways to learn about the variations of the insect on crops. The morphology methods may be divided into groups by features which are used by the methods. The features can be such as shape, structure, color, pattern or size of the object. In the aim to study the potential links between these variations and agricultural ecosystems, a set of beetles has been collected with all informations about the sex,

place where they were found and agricultural practices in each field were recorded. For each beetle, morphometric landmarks have been manually set on the images of the left and right mandibles. The morphometric landmarks are points precisely defined by biologists. Landmarks are widely used in many biological studies and they are currently included into the classification procedures.



(a) Left mandible (b) Right mandible

Permission to make digital or hard copies of all or part of this work for personal or classroom use is granted without fee provided that copies are not made or distributed for profit or commercial advantage and that copies bear this notice and the full citation on the first page. To copy otherwise, or republish, to post on servers or to redistribute to lists, requires prior specific permission and/or a fee.

In this paper, we focus on a chain of algorithms to automatically identify landmarks on our 2D images. The method mainly includes three stages: firstly, we segment the shape of the mandible, then principal

component analysis iteration is used to register one model image with a scene, the translation and rotation between the two images are also determined; finally, the landmarks are estimated by a method using a SIFT descriptor.

In section 2, we present the steps of our method. All experiments and evaluations are then described in section 3.

## 2 METHOD

The problem to solve is to suppress the manual operation of setting landmarks on each image. To do that, we propose a workflow, including the segmentation of each image and a registration with a model image. The model image is chosen randomly from the images without broken mandibles. The figure 2 shows the steps of the workflow:

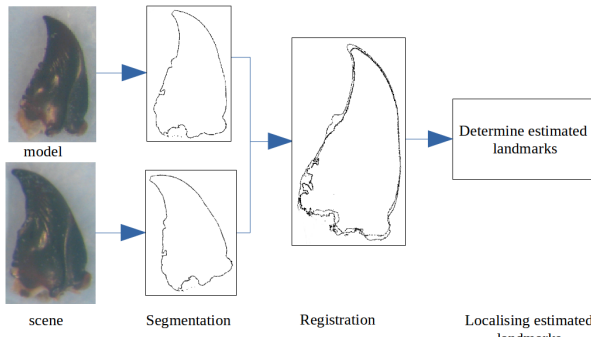


Figure 2: Overview of the proposed method

In this section, we will describe the different algorithms that we have used. It is worth to note that all pictures of mandibles have been taken in the same conditions with the same camera at the same resolution.

### 2.1 Image segmentation

Segmentation is often the first major task of an image processing chain. The most well-known algorithms are classified as contour or region based approaches. We have chosen a contours one, the Canny algorithm [2], allowing to determine the list of edges belonging to the shape of the image. To use this method, two threshold values have to be set. As it is often mentioned, determine the right values for these thresholds could be difficult[3]. The mandatory *threshold value* used by Canny algorithm has been determined by analyzing the image histogram (see [4] for detail). Most often authors define from this threshold, a lower and an upper one. The usual ratio of these two thresholds is  $T_{lower} = (1/2) * T_{upper}$ . In order to consider a larger range of values, we have prefer to set  $T_{lower}$  to 1/3 of

$T_{upper}$ . For optimization the computing time, the gradient direction of each pixel which belongs to the contours is computed during the Canny algorithm to be used later.

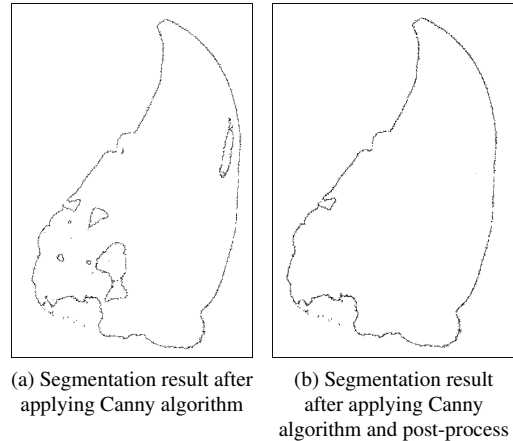


Figure 3: The segmentation results of the image

To achieve the segmentation, the obtained contours are post-processed to remove unnecessary ones. As it is shown in figure 3, the final result of Canny generates some contours which do not belong to the shape of the mandible. With a simple algorithm, we browse the image and suppress the edges inside the main shape.

### 2.2 Image registration

As mentioned, all images have been captured following the same protocol at the same scale. But it remains differences in size between the mandibles cause of size of the beetles, or orientation and position because of the mandible position under the camera. The next step concerns registration of model and scene before estimating the landmarks. Principal Component Analysis (PCA) is a well-known method to find the rotation and translation parameter values between two images. In our workflow, we have first used a classical PCA computing [7], [8].

As input values, we use the lists of points which have been defined by the segmentation step. Firstly, the centroid point and principal axis of each image are defined: the centroid point is the point which has the coordinate equal to the mean coordinate of all boundary points; the principal axis is a connected line from the centroid point to a point in the list of contours points which is determined as detailed in algorithm 1:

The translation is calculated by the distance of the centroid point of the scene and the model. The rotation angle is the angle between the principal axes of these two images. Then, the scene is moved to be register with the model. However, in some cases, the translation and rotation between two images are not enough

**Algorithm 1:** The algorithm for finding the principal axis of a list of contour points

---

**Input :** Centroid point, list points of contours  
**Output:** The principal axis

```

1 for all points i in the list of contour points do
2   Draw line l between i and centroid point;
3   for all points j in the list of contour points do
4     if i ≠ j then
5       Compute the perpendicular distance  $P_d$ 
          between line l and point j;
6     end
7   end
8   Compute the average ( $P_{mi}$ ) of all  $P_d$ ;
9   if  $P_{mi}$  is minimal then
10    | Store i as  $i_{min}$ ;
11   end
12 end
13 The principal axis is the line between centroid and  $i_{min}$ .

```

---

precise because the result of the segmentation could be not perfect. To improve registration, we have enhanced the PCA by iteration steps (PCAI). We have considered some specificity of our images and observed that the tip of mandible is less noisy than the base. So, we sort the points according to their y-value. We build a subset of points which contains half part of points, these ones belonging to the upper part of the image. PCA is again completed for this subset to refine the rotation and translation values. This operation is iterated until the new computing angle is less than 1.5 degree (see figure 4).

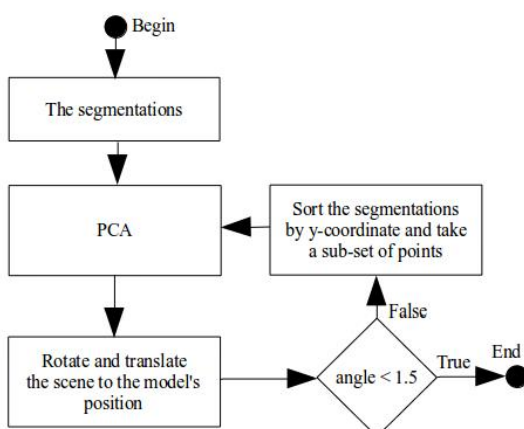


Figure 4: The flows in PCAI

Figure 5 shows an example of obtained results from the different steps of PCAI. In this figure, the red contours is the model segmentation, the black contours is the scene segmentation after one iteration, and the blue contours is the last result of PCAI .

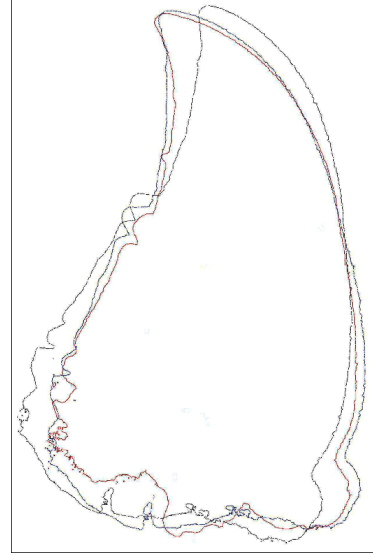


Figure 5: Different registration steps between two images

### 2.3 Localising the estimated landmarks

The last task of the workflow consists to estimate the landmarks of the scene from the manual ones of the model. We use SIFT [5] method. But we do not consider all points of the image as usually, only the area around the landmarks. Firstly, the region around each manual landmark (called patch) in the model is extracted and its corresponding position in the scene image is defined. Then, the SIFT descriptor is computed: the orientation and gradient magnitude are calculated for each pixel by using the gradient values computed at the Canny step and applying the equations (1):

$$\begin{aligned}
 m(x,y) &= \sqrt{P_x^2 + P_y^2} \\
 \theta(x,y) &= \tan^{-1}(P_y/P_x) \\
 (P_x &= P(x+1,y) - P(x-1,y) \text{ and} \\
 P_y &= P(x,y+1) - P(x,y-1))
 \end{aligned} \tag{1}$$

Where:

- $P(x,y)$  is the gray value at position  $(x,y)$  in the patch,
- $m(x,y)$  is the gradient magnitude of the pixel at position  $(x,y)$ ,
- $\theta(x,y)$  is the orientation of the pixel at position  $(x,y)$ .

The SIFT descriptor for each patch is an histogram which contains the sum of pixels gradient for each considering direction. As usually, eight directions are take into account ( $0^\circ - 45^\circ$ ,  $46^\circ - 90^\circ$ ,  $91^\circ - 135^\circ$ ,  $136^\circ - 180^\circ$ ,  $181^\circ - 225^\circ$ ,  $226^\circ - 270^\circ$ ,  $271^\circ - 315^\circ$ ,  $316^\circ - 360^\circ$ ). Finally, the feature vector is normalized to reduce the effects of illumination changes.

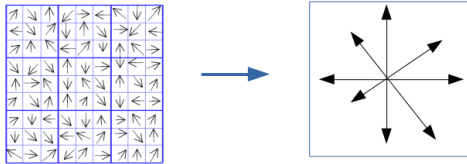


Figure 6: Calculus of the global descriptor for a patch.  
Gradient value is arrow length in the right figure

The figure 6 shows sample of a patch of 9x9 pixels created around each landmark on the model. The landmark of the model is located in the center of the patch. The size of 9x9 has been retained after several tests. Patch sizes: 18x18, 36x36, 54x54 have been also computed and gave us results statistically worst. From the histogram of the patch, we obtained the global gradient value for each direction.

The comparison between two SIFT descriptors is done by using  $L_2$  distance, equation (2).

$$L(D1, D2) = \sum_{i=0}^n \sqrt{(D1_i - D2_i)^2} \quad (2)$$

Where:

- $n$  is the number of directions
- $D1$  and  $D2$  are two descriptors with size  $n$ ,
- $D1_i, D2_i$  are the value at the location  $i$  in each descriptor.

Figure 7 illustrates how we apply SIFT into our work. To fix model landmarks on the scene, the patches  $P_m$ ,  $P_s$  are created with  $\text{size}(P_m) < \text{size}(P_s)$ . After experiments, we keep 36 (pixels) as the size of  $P_s$ . For each pixel in the patch  $P_s$ , a sub-patch  $P'_s$  is extracted with the same size than  $P_m$ . When the  $P'_s$  is not possible to get from  $P_s$  (border limits), the pixels outside  $P_s$  are more considered. Then, the distance  $L(P_m, P'_s)$  is computed by (2). This process is finished when all the pixels on the patch  $P_s$  are considered. The coordinates of an estimated landmark is the location in  $P_s$  that has the smallest measure distance value with  $P_m$ . Finally, the coordinates of the estimated landmarks are set to the original location of the scene by applying the reverse operation of rotation and translation.

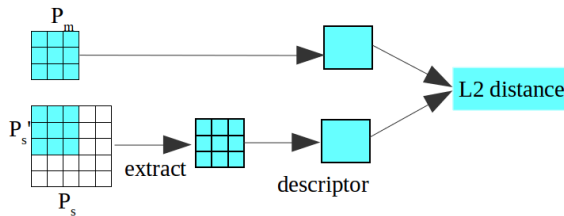


Figure 7: Illustrate the steps of descriptors comparison.

### 3 EXPERIMENTS AND RESULT

All the steps of our method are implemented in MAE-Lab<sup>1</sup>. The set of beetles has been analyzed, right and left mandibles. After verifying the quality of the image, it remains 290 usable images of right mandible and 286 images of the left mandible. The removed images include the images that do not contain the mandible or the broken mandibles. In all valid images, a set of manual landmarks are indicated by biologists: 18 for right mandibles, 16 for left mandibles.

We have run the full workflow on all images. The preliminary results have shown differences in algorithm accuracy: estimated landmarks are well positioned on some scenes but not satisfying on others. As we mentioned before, mandibles can exhibit different sizes because beetles have also. It seems that our method is sensible to this parameter. To improve our results, we have inserted a step before computing SIFT descriptor to estimate the scale between one scene image and the model. The bounding boxes of the mandible of the model image and the scene image are computed and the scales of x and y-direction are determined by the ratio between the corresponding sides of the bounding boxes. Then, the scene contours are scaled to fit the model contours.

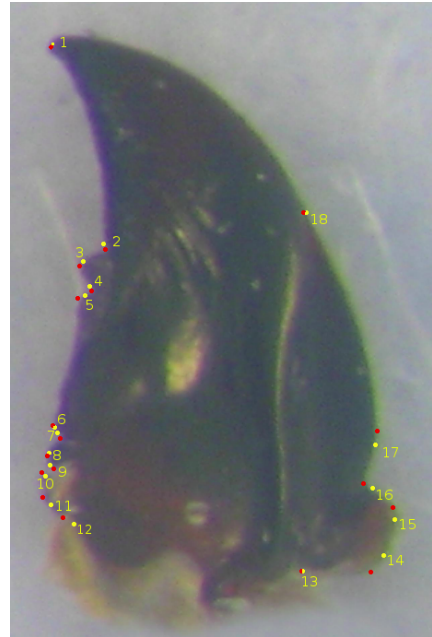


Figure 8: The manual and estimated landmarks on right mandible

<sup>1</sup> MAELab is a free software in C++. It can be directly obtained by request the authors.

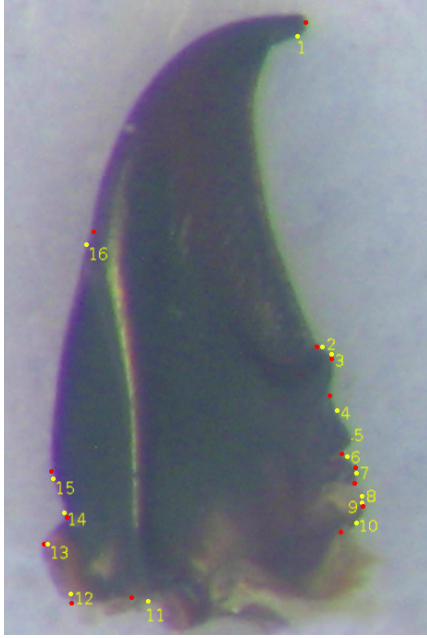


Figure 9: The manual and estimated landmarks on left mandible

Figure 8 and 9 show complete results on one right mandible and one left mandible with the manual landmarks (red points) and estimated landmarks (yellow points). The estimated landmarks are quite near with the manual landmarks. This shows that our method works well for indicating the landmarks on the mandibles.

In the evaluation, the statistic is done on all landmarks of the images. We have compared the coordinates between the manual and estimated landmarks and accept the error in the range between 1% to 2% of the bounding box's size. According to this way, a global statistic compares all pairs of landmarks (manual and corresponding estimated landmarks) on all images.

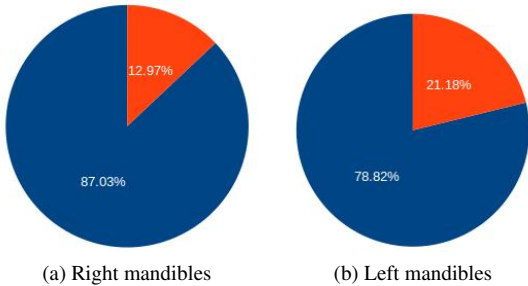


Figure 10: The global proportions of well and bad landmark locations on the mandibles

Figure 10 shows the global results: we have obtained **87.03%** for right mandibles and **78.82%** for left mandibles of well positioned estimated landmarks.

Besides the global results, we are also interested in the accuracy of the individual position of the estimated landmarks. We have computed the distance between the manual and corresponding estimated landmarks in order to examine the correct proportion on each landmark and think about replacing the manual landmarks by corresponding estimated landmarks.

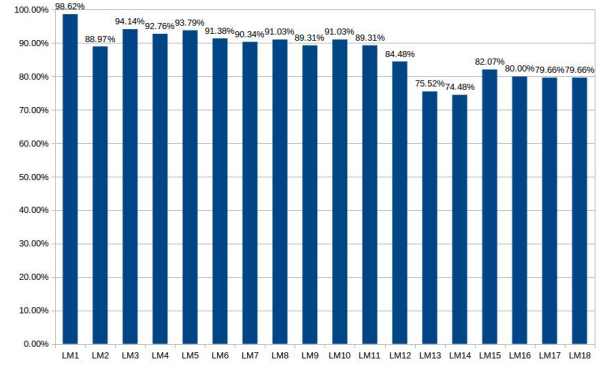


Figure 11: The correct proportions on each landmark of right mandibles

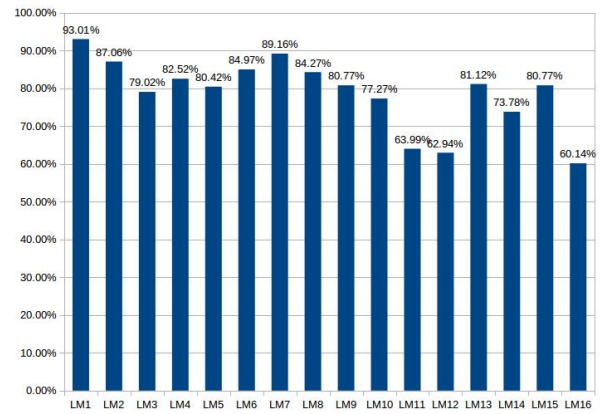


Figure 12: The correct proportions on each landmark of left mandibles

Figure 11 and 12 show the correct proportion on each landmark of the mandibles. With 18 landmarks of right mandible, the position of the first estimated landmarks is reasonably accurate with **98.62%**, the lowest proportion is **74.48%** for fourteenth landmark. The remaining landmarks are also indicated with a high proportion (with the accuracy proportion greater than 75%). For left mandible, the highest and lowest success rate are **93.01%** for the first landmark and **60.14%** for the sixteenth landmark. The statistic is done on each estimated landmarks of all the images with a standard deviation error [1]. As we can see in figure 3, the noise of the contour part located at the base of mandible is higher than the noise located at the tip of the mandible. This explains why the correct proportion on 11<sup>th</sup>, 12<sup>th</sup> landmark of the left mandible or 13<sup>th</sup>, 14<sup>th</sup> landmark

of the right mandible are less than other landmarks. Moreover, when we reconsider the datasets, the images in left mandible have a higher number of scales than on the right mandible. This explains the success rate on the right mandible is always greater than the left mandible in both of the experiments.

From two experiment ways, we can see that the method succeeded in locating all landmarks for each image; and the found location of the landmarks can be considered as ground-truth like the manual ones. Moreover, considering the previous work in [4], this method reduces the drastically the number of outlier landmarks. In MAELab implementation, we also reduce the computing time and memory cost.

## 4 CONCLUSION

Morphometric analysis is a powerful tool in biology for the species classification. In the content of this paper, we have begun to design a method to segment the beetle mandibles and automatically locate landmarks which have been determined by biologists. Each mandible is segmented by applying the Canny algorithm. Using PCAI to align the images. Finally, the estimated landmarks are indicated by applied SIFT descriptor. The results show that in order to replace the manual landmarks, the estimated landmarks are accuracy enough. MAELAb library proposes a efficient implementation of this method. From now, the next stage consists in improving the registration step in order to increase the matching step accuracy. By example, we would investigate the isomorphic of registration methods.

## 5 REFERENCES

- [1] J Martin Bland and Douglas G Altman. Statistics notes: measurement error. *Bmj*, 313(7059):744, 1996.
- [2] John Canny. A computational approach to edge detection. *Pattern Analysis and Machine Intelligence, IEEE Transactions on*, (6):679–698, 1986.
- [3] Dehua Li Jun Zeng. An adaptive canny edge detector using histogram concavity analysis. *International Journal of Digital Content Technology and its Applications*, 5, 2011.
- [4] L Lê Vănh, M Beurton-Aimar, JP Salmon, A Marie, and N Parisey. Estimating landmarks on 2d images of beetle mandibles. *WSCG*, 2016.
- [5] David G Lowe. Distinctive image features from scale-invariant keypoints. *International journal of computer vision*, 60(2):91–110, 2004.
- [6] Sasirekha Palaniswamy, Neil A Thacker, and Christian Peter Klingenberg. Automatic identification of landmarks in digital images. *IET Computer Vision*, 4(4):247–260, 2010.
- [7] K. Pearson. On lines and planes of closest fit to systems of points in space. *Philosophical Magazine*, 2(6):559–572, 1901.
- [8] Jonathon Shlens. A tutorial on principal component analysis. *arXiv preprint arXiv:1404.1100*, 2014.